

Modern theory of nuclear forces

Ulf-G. Meißner^{a, b}

^aUniversität Bonn, Helmholtz-Institut für Strahlen- und Kernphysik (Th)
D-53115 Bonn, Germany

^bForschungszentrum Jülich, Institut für Kernphysik (Th)
D-52425 Jülich, Germany

Nuclear forces can be systematically derived using effective chiral Lagrangians consistent with the symmetries of QCD. I review the status of the calculations for two- and three-nucleon forces and their applications in few-nucleon systems. I also address issues like the quark mass dependence of the nuclear forces and resonance saturation for four-nucleon operators.

1. INTRODUCTION

The forces between two (a few) nucleons is one of the most studied problems in theoretical physics. Over many decades, a standard picture had evolved, in which these forces are described in terms of meson exchanges (which is an extension of the range expansion suggested in the 1950ties by Taketani and collaborators [1]). Nuclei, which comprise most of the baryonic matter in the universe, are made of slowly moving nucleons, so that given a potential, one simply has to solve the Schrödinger equation for the A -nucleon system,

$$H\psi_A = E\psi_A \tag{1}$$

to obtain the properties of nuclei. More precisely, the nuclear Hamiltonian can be written as

$$H = T + V, \quad V = \sum_{i \neq j} V_{ij} + \sum_{i \neq j \neq k} V_{ijk} + \dots, \tag{2}$$

with T the kinetic energy operator and the potential V is a string of terms comprising two- and three-nucleon forces. Given the two-nucleon potential V_{ij} obtained e.g. from the analysis of the many NN scattering data and adjusting a few parameters in the three-nucleon potential V_{ijk} , the spectra for nuclei up to $A \simeq 12$ (and other properties) can be calculated with high precision using Monte-Carlo methods leading to an astonishing agreement with data (see e.g. [2, 3]). Other precision methods exist for few-nucleon systems, like e.g. exact solutions of the Faddeev-Yakubovsky equations, the stochastic variational method or the use of hyperspherical harmonics. However, in such a framework based on meson exchange or semi-phenomenological potentials, one can not explain why the $2N$ forces are so much stronger than the $3N$ ones and also, when including external

sources, gauge invariance is not easy to obey (but there are prescriptions to do so). Furthermore, the connection to the fundamental theory of the strong interactions, QCD, is loose and it is difficult to estimate the theoretical errors. On the other hand, over the last few decades Chiral Perturbation Theory (CHPT) has become a standard tool for analyzing the properties of hadronic systems at low energy where the perturbative expansion of QCD in powers of the coupling constant cannot be applied. It is based on the approximate and spontaneously broken chiral symmetry of QCD. Starting from the most general effective Lagrangian for Goldstone bosons (pions in the two-flavor case of u and d quarks) and matter fields (nucleons, ...) consistent with the symmetries of QCD, the hadronic S-matrix elements are obtained via a simultaneous expansion in small external momenta and quark masses (where small refers to the scale of symmetry breaking, $\Lambda_\chi \simeq 1 \text{ GeV}$). Goldstone boson loops are incorporated to obey perturbative unitarity and all corresponding ultraviolet divergences can be absorbed at a given order in the chiral expansion by the counterterms of the effective Lagrangian. This perturbative scheme works well in the pion and the pion-nucleon sectors, where the interaction vanishes when the external momenta go to zero (in the chiral limit). In the case of a few interacting nucleons, the situation is very different in that one has to deal with a non-perturbative system. Indeed, perturbation theory is expected to fail already at low energy due to the presence of the shallow few-nucleon bound states. To make this more precise, observe that the np scattering length in the 1S_0 partial wave is much bigger than the largest natural scale set by the pion Compton wavelength, $|a(^1S_0)| \simeq 24 \text{ fm} \gg 1/M_\pi \simeq 1.4 \text{ fm}$ or consider the binding momentum in the deuteron, which is much smaller than the pion mass, $\gamma = \sqrt{B_d m_d/2} \simeq 45 \text{ MeV} \ll M_\pi \simeq 140 \text{ MeV}$. A suitable non-perturbative approach has been suggested by Weinberg [4], who showed that the strong enhancement of the few-nucleon scattering amplitude arises from purely nucleonic intermediate states. Weinberg suggested to apply power counting to the kernel of the corresponding scattering equation, which can be viewed as an effective nuclear potential. This idea has been explored in the last decade by many authors. In the following I will show how far this program has matured in the description of few-nucleon systems. Space does not allow for giving an accurate representation of the historical developments and also I will not discuss the pionless effective field theory (EFT) here (for comprehensive reviews see [5, 6]).

2. EFFECTIVE CHIRAL LAGRANGIAN

Here I briefly discuss the effective chiral Lagrangian \mathcal{L}_{eff} underlying the EFT calculation of the nuclear forces. The QCD Lagrangian for massless up and down quarks is invariant under global flavor $SU(2)_L \times SU(2)_R$ transformations or, equivalently, under vector and axial-vector transformations. This is called chiral symmetry. Among other facts, the absence of parity doublets of low mass hadrons suggests that the axial symmetry is spontaneously broken. The pions are the natural candidates for the required Goldstone bosons. They acquire a non-vanishing mass due to the explicit symmetry breaking caused by the small up and down quark masses. We are interested in low-energy nuclear physics here, where the degrees of freedom are the composite hadrons. Their interaction can be described by an effective Lagrangian, which has to be constrained by chiral symmetry and should include explicitly symmetry breaking parts proportional to powers of the quark

masses (for the relation between the effective chiral Lagrangian and QCD, see [7, 8]). For the applications to be considered, nucleon momenta are comparable to the pion mass and somewhat higher, but still smaller than the ρ -mass. In that case a standard one-boson exchange picture turns into NN contact forces for the heavy meson exchanges and only the few-pion exchanges are kept explicitly. The construction of the most general effective Lagrangian out of pion and nucleon fields constrained by chiral symmetry is by now standard, based on the non-linear realization of chiral symmetry. There is an infinite number of possible terms, which can be ordered according to the parameter

$$\Delta = d + \frac{1}{2}n - 2 \quad (3)$$

characterizing the vertices (note this differs from the standard counting done in the pion and pion-nucleon sectors). Here d is the number of derivatives and n the number of nucleon field operators. Spontaneously broken chiral symmetry enforces $\Delta \geq 0$. The first few terms for the interacting effective Lagrangian after a p/m expansion take the form (for an early detailed review on the construction principles and applications, see [9])

$$\begin{aligned} \mathcal{L}_{\text{eff}}^{(0)} &= -N^\dagger \left[\frac{g_A}{2F_\pi} \boldsymbol{\tau} \boldsymbol{\sigma} \cdot \nabla \boldsymbol{\pi} + \frac{1}{4F_\pi^2} \boldsymbol{\tau} \cdot (\boldsymbol{\pi} \times \dot{\boldsymbol{\pi}}) + \dots \right] N \\ &\quad - \frac{1}{2} C_S (N^\dagger N) (N^\dagger N) - \frac{1}{2} C_T (N^\dagger \boldsymbol{\sigma} N) (N^\dagger \boldsymbol{\sigma} N) , \end{aligned}$$

$$\mathcal{L}_{\text{eff}}^{(1)} = + \frac{1}{F_\pi^2} N^\dagger \left[-2c_1 M_\pi^2 \boldsymbol{\pi}^2 + c_3 \partial_\mu \boldsymbol{\pi} \partial^\mu \boldsymbol{\pi} - \frac{1}{2} c_4 \varepsilon_{ijk} \varepsilon_{abc} \sigma_i \tau_a (\nabla_j \pi_b) (\nabla_k \pi_c) + \dots \right] N \quad (4)$$

$$- \frac{D}{4F_\pi} (N^\dagger N) (N^\dagger \boldsymbol{\sigma} \cdot \boldsymbol{\tau} N) \cdot \nabla \boldsymbol{\pi} - \frac{1}{2} E (N^\dagger N) (N^\dagger \boldsymbol{\tau} N)^2 , \quad (5)$$

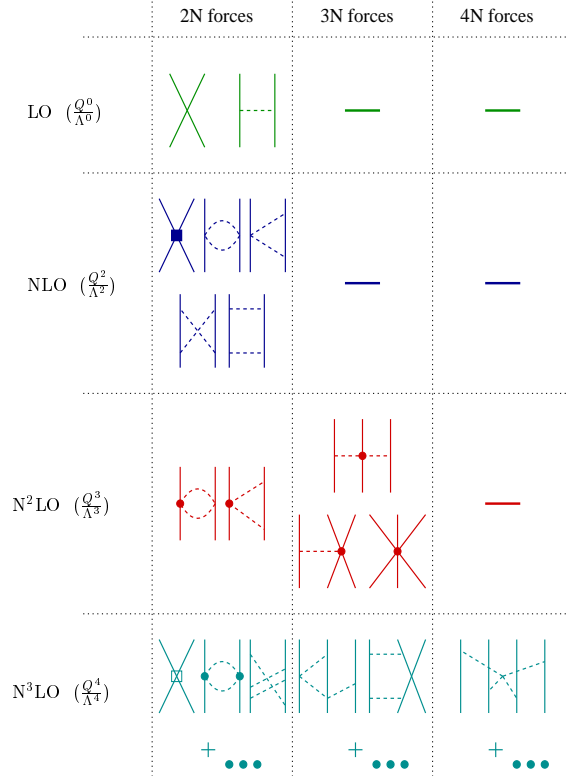
$$\mathcal{L}_{\text{eff}}^{(2)} = - \frac{1}{2} C_1 [(N^\dagger \nabla N)^2 + (\nabla N^\dagger N)^2] + \dots + C_7 (\partial_i N^\dagger \sigma_i \partial_i N) (N^\dagger \sigma_i N) + \dots , \quad (6)$$

where the upper index refers to $\Delta = 0, 1$ and 2 . Here, N and $\boldsymbol{\pi}$ denote the isodoublet nucleon and the isovector pion fields, in order. The parameters of \mathcal{L}_{eff} , the so called low-energy constants (LECs), can be partitioned in several groups: some can be determined in the π/π -N system ($g_A, F_\pi, c_1, c_3, c_4$) and others from nucleonic systems only ($C_S, C_T, E, C_1, \dots, C_7$). The constant D also affects the NN π system, see [10]. All these constants are of course not determined by chiral symmetry, but have to be adjusted to experimental data.

3. THE HIERARCHY OF NUCLEAR FORCES

The strength of the EFT approach is based on its underlying power counting, which allows to organize all possible contributions to the N -nucleon potential in a systematic way. As a consequence of that, one naturally obtains a hierarchy of nuclear forces, as was shown already by Weinberg [4] and van Kolck [11]. Here, I will discuss how this comes about including corrections at next-to-next-to-next-to-leading order ($N^3\text{LO}$). According to chiral power counting the dominant contributions to the effective Hamiltonian for few nucleons are of the order $(Q/\Lambda)^0$, where $Q \sim M_\pi$ refers to the soft scale (typical momenta involved in the process) and Λ to the hard scale (the chiral symmetry breaking scale, or

Figure 1. The hierarchy of the nuclear forces in chiral effective field theory. Shown are representative diagrams (contact interactions, one-, two- and three-pion exchanges) symbolizing the various topologies at leading, next-to-leading, ... order. Due to parity, $2N$ contact interactions can only appear at even orders in Q/Λ . The two-pion exchange diagrams at $N^2\text{LO}$ ($N^3\text{LO}$) include couplings with two (three) derivatives (or pion mass insertions) from the πN effective chiral Lagrangian. At $N^3\text{LO}$, only a few topologies are shown as indicated by the ellipsis.



the ultraviolet cut-off to render the scattering equation finite). These leading-order (LO) contributions turn out to be of the $2N$ type, given by one-pion exchange (OPE) and two four-nucleon contact interactions without derivatives, cf. Fig. 1. The first corrections at next-to-leading order (NLO) are of the order $(Q/\Lambda)^2$ and still of the $2N$ type. They result from two-pion exchange (TPE) with the leading (i.e. with one derivative) πNN and $\pi\pi NN$ vertices and seven independent NN contact interactions with two derivatives. The LECs entering the expressions for TPE at NLO are the nucleon axial-vector coupling g_A and the pion decay constant F_π . Both LECs are measured rather accurately, so that the leading TPE contribution is parameter-free. On the contrary, the LECs accompanying the four-nucleon contact operators are unknown and have to be fixed from a fit to low angular momentum partial waves. Thus, at LO and NLO we have only two-nucleon forces and therefore expect more-nucleon forces to be parametrically suppressed, in agreement with empirical information.

At NNLO ($\sim (Q/\Lambda)^3$) one has to take into account the subleading TPE contributions given by the triangle diagram with the $\pi\pi NN$ vertex with two derivatives or one insertion of M_π^2 . The corresponding LECs are denoted $c_{1,3,4}$ and have been fixed in the πN system, see e.g. [12, 13, 14]. The numerical values of these LECs found in several analyses of πN scattering in CHPT are rather large compared to what is expected on dimensional reasons. Similar large values of $c_{3,4}$ have also been obtained recently from the np and pp partial wave analysis carried out by the Nijmegen group [15]. The large values of the $c_{3,4}$ can at least be partially explained by the fact that these LECs are saturated by the Δ -excitation [12]. Other important contributions to c_1 and c_4 can be traced back to meson-exchange

in the t -channel. The large numerical values of the c_i 's gives rise to a subleading TPE contribution to the NN potential that shows an unphysically strong attraction already at intermediate distances $r \sim 1 - 2$ fm when standard dimensional regularization in the pion loop integrals is applied. This was already pointed out in Ref. [16]. To circumvent this problem, spectral function regularization was proposed in [17], as explained in the next section. It is important to note that at this order the first non-vanishing three-nucleon forces (3NF) appear, given by the three topologies shown in Fig. 1. I will come back to these later. Finally, at N³LO, one has to consider four-nucleon terms with four derivatives (or pion mass insertions), further corrections to the two-pion exchange (including now some of the dimension three couplings d_i from $\mathcal{L}_{\text{eff}}^{(2)}$) as well as the leading order three-pion exchange. These TPE and 3PE corrections were worked out explicitly utilizing DR in [18]. For the NN problem, one has 15 independent four-nucleon operators that feed into the S-, P- and D-waves and the corresponding mixing angles. Further corrections to the 3NF also appear at this order, it is however very important to stress that these are free of unknown six-nucleon LECs. In addition, the first non-vanishing corrections to the four-nucleon force appear at this order. Consequently, assuming that all coefficients are of natural size, chiral symmetry applied to the few-nucleon potential gives the hierarchy of the forces

$$\langle V_{2N} \rangle_A \gg \langle V_{3N} \rangle_A \gg \langle V_{4N} \rangle_A , \quad (7)$$

which is in agreement with phenomenological determinations of these forces.

4. SPECTRAL FUNCTION REGULARIZATION

Before discussing the physics related to few-nucleon systems, there is one important technical development to be discussed in a bit of detail here. As already stated, the numerically large values of the LECs c_i found in the πN system lead to an unphysically strong attraction of subleading TPE. This is related to the use of dimensional regularization in the pion loop integrals. This problem can be overcome employing spectral function regularization, which has been used early in the construction of two-pion exchange contributions to the NN potential based on dispersion theory [19]. To be specific, consider the isoscalar central part of the subleading TPE which results from the triangle diagram and is given by

$$V_C(q) = \frac{3g_A^2}{16F_\pi^4} \int \frac{d^3l}{(2\pi)^3} \frac{l^2 - q^2}{((\vec{q} - \vec{l})^2 + 4M_\pi^2)((\vec{q} + \vec{l})^2 + 4M_\pi^2)} (8c_1 M_\pi^2 + c_3(l^2 - q^2)) , \quad (8)$$

where \vec{q} is the nucleon momentum transfer and $q \equiv |\vec{q}|$, $l \equiv |\vec{l}|$. The integral is cubically divergent and needs to be regularized. Applying dimensional regularization (DR) one finds:

$$V_C(q) = -\frac{3g_A^2}{16\pi F_\pi^4} (2M_\pi^2(2c_1 - c_3) - c_3 q^2) (2M_\pi^2 + q^2) \frac{1}{2q} \arctan \frac{q}{2M_\pi} + \dots . \quad (9)$$

The ellipses refer to polynomial terms of the kind $\alpha + \beta q^2$, whose explicit form is not of relevance here. In order to obtain the potential in coordinate space one has to make an inverse Fourier-transform of $V_C(q)$ in Eq. (9). The ordinary inverse Fourier-transform is

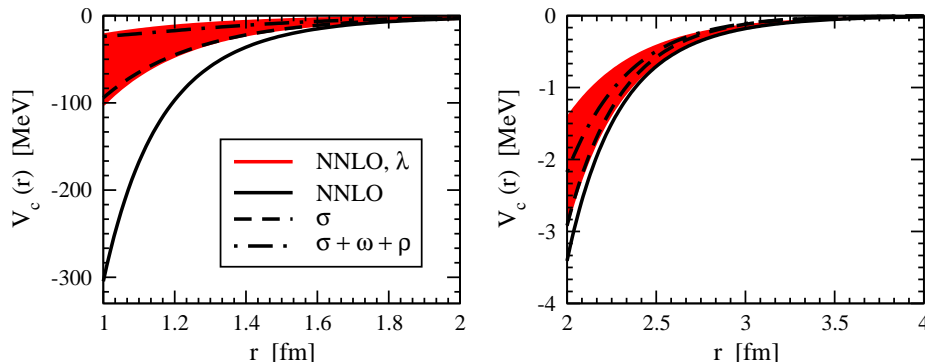


Figure 2. The potential V_C in r -space. The solid line (shaded band) shows the DR (spectral function regularized, $\lambda = 500 \dots 800$ MeV) result. The dashed (dashed-dotted) line refers to the phenomenological σ ($\sigma + \omega + \rho$) contributions based on the isospin triplet configuration space version (OBEPR) of the Bonn potential.

obviously not possible due to the fact that $V_C(q)$ grows with q . One can nevertheless obtain $V_C(r)$ at each $r > 0$ using the spectral function representation [16]:

$$V_C(q) = \frac{2q^4}{\pi} \int_{2M_\pi}^{\infty} d\mu \frac{1}{\mu^3} \frac{\rho(\mu)}{\mu^2 + q^2}, \quad (10)$$

where the spectral function $\rho(\mu)$ can be obtained from $V_C(q)$ in Eq. (9) via

$$\rho(\mu) = \Im [V_C(0^+ - i\mu)] = -\frac{3g_A^2}{64F_\pi^4} (2M_\pi^2(2c_1 - c_3) + c_3\mu^2) (2M_\pi^2 - \mu^2) \frac{1}{\mu} \theta(\mu - 2M_\pi). \quad (11)$$

In eq. (10) a twice subtracted dispersion integral is given which is needed in order to account for the large- μ behavior of $\rho(\mu)$.

The inverse Fourier-transform in terms of the spectral function $\rho(\mu)$ can easily be evaluated via

$$V_C(r) = \frac{1}{2\pi^2 r} \int_{2M_\pi}^{\infty} d\mu \mu e^{-\mu r} \rho(\mu). \quad (12)$$

Substituting $\rho(\mu)$ from Eq. (11) into Eq. (12) and using for the LECs $c_{1,3}$ the central values from [14], $c_1 = -0.81 \text{ GeV}^{-1}$ and $c_3 = -4.70 \text{ GeV}^{-1}$, one obtains the coordinate space representation of the potential $V_C(r)$ shown by the solid line in Fig. 2. The central part of the NNLO TPE potential turns out to be several times more attractive at intermediate distances than the phenomenological σ ($\sigma + \omega + \rho$) contributions. This unphysical attraction shows up in the D- and F-wave phase shifts as observed in [16]. The origin of the unphysical attraction at NNLO can be traced back by looking at the integral in Eq. (12). While at large distances the integral is dominated by low- μ components (of the order $\mu \sim 350$ MeV), already at intermediate distances rather high- μ terms (of the order $\mu \sim 600$ MeV) in the spectral function provide a dominant contribution. Clearly, at shorter distances even higher- μ components become important. Chiral EFT can hardly provide convergent results for the spectral function at $\mu \sim 600$ MeV and higher. Instead

of keeping such large- μ contributions in the regularized loop integral expressions it is advantageous to perform the integration in Eqs. (10,12) only over the low- μ region, where chiral EFT is applicable. This can be achieved by introducing the regularized spectral function

$$\rho(\mu) \rightarrow \rho^\lambda(\mu) = \rho(\mu) \theta(\lambda - \mu), \quad (13)$$

with the reasonably chosen cut-off $\lambda < M_\rho$. Certainly, taking a too small λ in Eq. (13) will remove the truly long-distance physics while too large values for the cut-off may affect the convergence of the EFT expansion due to the inclusion of spurious short-distance physics. In Fig. 2 we show $V_C(r)$ obtained using the spectral function regularization Eq. (13) with $\lambda = 500 \dots 800$ MeV. The strongest effects of the cut-off are observed at intermediate and short distances, where the unphysical attraction in dimensionally regularized TPE is greatly reduced. On the other hand, the asymptotic behavior of the potential at large r is not affected by the choice of regularization. The results for D- and F-waves are greatly improved when the spectral function regularization is used instead of DR, see [17]. One can also show that the spectral function regularization is equivalent to (finite) momentum cut-off regularization of pion loop integrals. It should be understood that this new regularization scheme does not introduce any model dependence in the EFT procedure as soon as λ is chosen of the order of (or larger than) M_ρ . Various choices for λ (including $\lambda = \infty$, which is equivalent to DR) differ from each other by higher-order contact terms and lead to exactly the same result for observables provided one keeps terms in all orders in the EFT expansion. Of course, this choice of regularization in Eq. (13) is by no means unique. Different choices lead to equivalent results for the potential up to higher order terms and may be used as well. The advantage of the form Eq. (13) is that it does not generate spurious long-range contributions which are suppressed by inverse powers of λ . For a more detailed discussion on this issue, I refer to [17].

5. TWO NUCLEONS AT N³LO

The interactions between two nucleons at N³LO were studied in [20]. Here, I can only sketch the most salient features of that study. As discussed before, at this order the two-nucleon potential consists of one-, two- and three-pion exchanges and a set of contact interactions with zero, two and four derivatives, respectively. We have applied spectral function regularization to the multi-pion exchange contributions. Within this framework, we have shown that three-pion exchange can safely be neglected. The corresponding cut-off is varied from 500 to 700 MeV. The LECs related to the dimension two and three $\bar{N}N\pi\pi$ vertices are taken consistently from studies of pion-nucleon scattering in chiral perturbation theory [13, 14]. In the isospin limit, there are 24 LECs related to four-nucleon interactions which feed into the S-, P- and D-waves and various mixing parameters. In addition, various isospin breaking mechanisms were considered. In the actual calculations, we have included the leading charge-independence and charge-symmetry breaking four-nucleon operators, the pion and nucleon mass differences in the 1PE, and the same electromagnetic corrections as done by the Nijmegen group (the static Coulomb potential and various corrections to it, magnetic moment interactions and vacuum polarization). This is done because we fit to the Nijmegen partial waves. In the future,

it would be important to also include mass differences in the 2PE, $\pi\gamma$ -exchange and the isospin breaking corrections to the pion-nucleon scattering amplitude (which have been consistently determined in [21]). We therefore have phases for the pp , np and nn systems. To obtain the bound and scattering states, we use the Lippmann-Schwinger equation with the relativistic form of the kinetic energy. Such an approach can easily be extended to external probes or few-nucleon systems. The LS equation is regulated in the standard way, namely by multiplying the potential $V(\vec{p}, \vec{p}')$ with a regulator function f^Λ ,

$$V(\vec{p}, \vec{p}') \rightarrow f^\Lambda(p) V(\vec{p}, \vec{p}') f^\Lambda(p'). \quad (14)$$

We use the exponential regulator function $f^\Lambda(p') = \exp[-p^6/\Lambda^6]$, with the cut-off varied from 450 to 600 MeV. The total of 26 four-nucleon LECs has been determined by a combined fit to some np and pp phase shifts from the Nijmegen analysis together with the nn scattering length value $a_{nn} = -18.9$ fm. The resulting LECs are of natural size except $D_{1S_0}^1$ and $D_{3S_1}^1$. In contrast to the fits at NLO and NNLO, we had to extend the fit range to $E_{\text{lab}} = 200$ MeV. The description of the low phase shifts (S, P, D) is excellent, see Fig. 3 for the S- and some selected P- and D-waves. In all cases, the N³LO

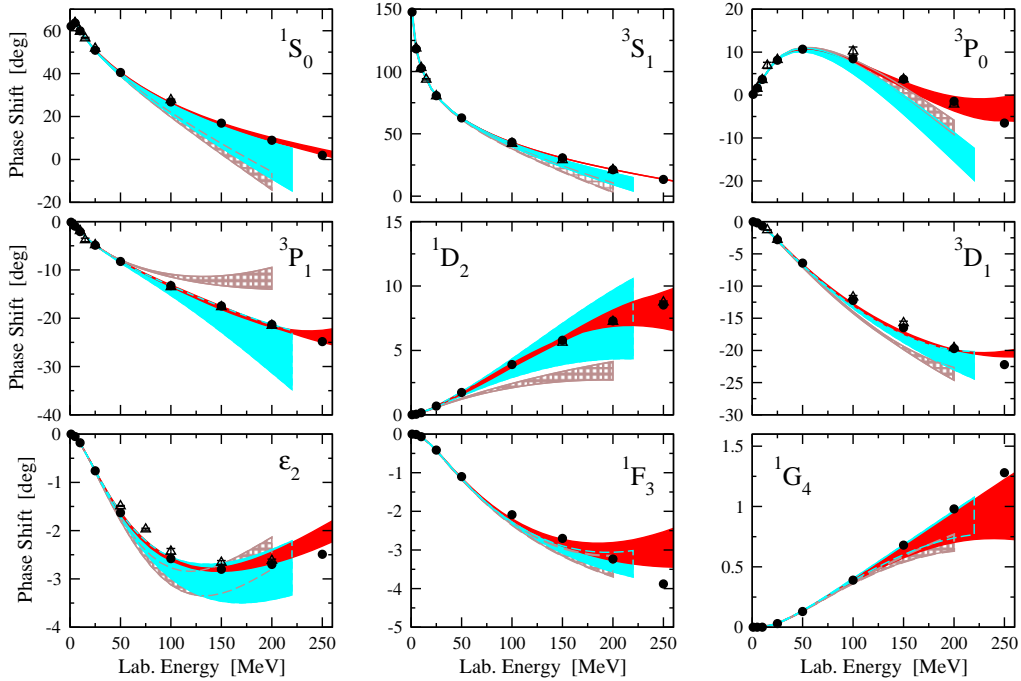


Figure 3. Selected np phase shifts and mixing angle ϵ_2 versus the nucleon laboratory energy. The grid, light shaded and dark shaded bands show the NLO, NNLO [17] and N³LO results, respectively. The filled circles depict the Nijmegen PWA results [22] and the open triangles are the results from the Virginia Tech PWA [23].

result is better than the NNLO one with a sizeably reduced theoretical uncertainty. This holds in particular for the problematic 3P_0 wave which was not well reproduced at NNLO. The peripheral waves (F, G, H, ...), that are free of parameters, are also well described with the expected theoretical uncertainty related to the cut-off variations, see Fig. 3 for

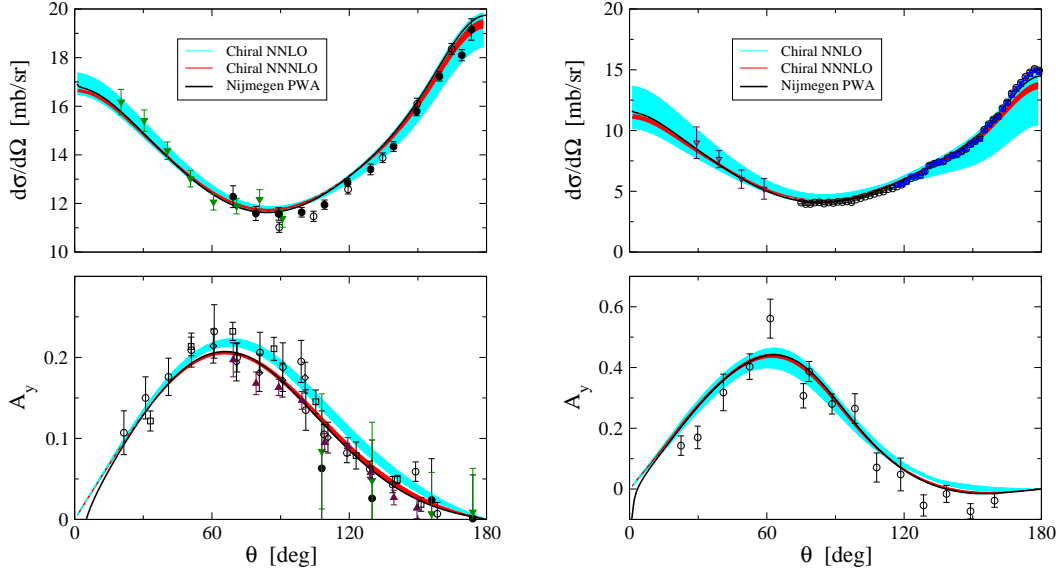


Figure 4. np differential cross section (upper row) and vector analyzing power (lower row) at $E_{\text{lab}} = 50$ MeV (left panel) and $E_{\text{lab}} = 96$ MeV (right panel). Shaded bands refer to the NNLO result, dashed lines to the Nijmegen phase shift analysis (NPSA) [22].

1F_3 and 1G_4 . We stress that the description of the phases in general improves when going from LO to NLO to NNLO to $N^3\text{LO}$, as it is expected in a converging EFT. The resulting S -wave scattering lengths and range parameters in the np and pp systems are in good agreement with the ones obtained in the Nijmegen PWA. In addition, we can give theoretical uncertainties for all these quantities, which are mostly in the one percent range. The scattering observables (differential cross sections, analyzing powers) for the np system as shown e.g. in Fig. 4 are well described, with a small theoretical uncertainty at the order considered here. The deuteron properties are further predictions. In particular, we have not included the binding energy in the fits, the deviation from the experimental value is in the range from 0.4 to 0.07%. The asymptotic S -wave normalization and the asymptotic D/S ratio are also well described, see Table 1. The remaining discrepancies in the quadrupole moment and the rms matter radius are related to the short-ranged two-nucleon current not considered in [20]. Note that the $2N$ system at this order was also studied in [24], utilizing dimensional regularization in the pion loop graphs. In that work, however, no detailed discussion of the theoretical uncertainties was given.

Table 1

Deuteron properties at various orders in chiral EFT in comparison to the data.

	NLO	$N^2\text{LO}$	$N^3\text{LO}$	Exp.
E_d [MeV]	-2.171 ... -2.188	-2.189 ... -2.202	-2.216 ... -2.223	-2.2246
A_S [$\text{fm}^{1/2}$]	0.868 ... 0.873	0.874 ... 0.879	0.882 ... 0.883	0.8846(9)
η	0.0256 ... 0.0257	0.0255 ... 0.0256	0.0254 ... 0.0255	0.0256(4)

6. THREE NUCLEONS AT N²LO

In the chiral EFT framework, three-nucleon forces (3NFs) arise consistently with the NN forces from the effective Lagrangian. This is one of the major advantages of this approach - such a consistency has never been achieved before. Furthermore, chiral EFT also allows to generate the most general structures consistent with the underlying symmetries, this is simply a consequence of utilizing the most general effective Lagrangian consistent with these principles. As noted earlier, the leading non-vanishing contributions to the 3NF appear at NNLO, given by three different topologies (see Fig. 1): the TPE graphs, the OPE diagram and the six-nucleon contact interactions. The TPE contribution is given in terms of LECs $c_{1,3,4}$ from the pion-nucleon system (see [25, 26])

$$V_{\text{TPE}}^{\text{3NF}} = \sum_{i \neq j \neq k} \frac{1}{2} \left(\frac{g_A}{2F_\pi} \right)^2 \frac{(\boldsymbol{\sigma}_i \cdot \mathbf{q}_i)(\boldsymbol{\sigma}_j \cdot \mathbf{q}_j)}{(\mathbf{q}_i^2 + M_\pi^2)(\mathbf{q}_j^2 + M_\pi^2)} F_{ijk}^{\alpha\beta} \tau_i^\alpha \tau_j^\beta, \quad (15)$$

where $\mathbf{q}_i \equiv \mathbf{p}_i' - \mathbf{p}_i$; \mathbf{p}_i (\mathbf{p}_i') are the initial (final) momenta of the nucleon i and

$$F_{ijk}^{\alpha\beta} = \delta^{\alpha\beta} \left[-\frac{4c_1 M_\pi^2}{F_\pi^2} + \frac{2c_3}{f_\pi^2} \mathbf{q}_i \cdot \mathbf{q}_j \right] + \sum_\gamma \frac{c_4}{F_\pi^2} \epsilon^{\alpha\beta\gamma} \tau_k^\gamma \boldsymbol{\sigma}_k \cdot [\mathbf{q}_i \times \mathbf{q}_j].$$

The OPE and contact contributions are given in terms of the LECs D and E , respectively, and take the form

$$V_{\text{OPE}}^{\text{3NF}} = - \sum_{i \neq j \neq k} \frac{g_A}{8F_\pi^2} D \frac{\boldsymbol{\sigma}_j \cdot \mathbf{q}_j}{\mathbf{q}_j^2 + M_\pi^2} (\boldsymbol{\tau}_i \cdot \boldsymbol{\tau}_j) (\boldsymbol{\sigma}_i \cdot \mathbf{q}_j), \quad (16)$$

$$V_{\text{cont}}^{\text{3NF}} = \frac{1}{2} \sum_{j \neq k} E (\boldsymbol{\tau}_j \cdot \boldsymbol{\tau}_k). \quad (17)$$

To pin down the 3NF at this order, one needs two observables to determine the LECs E and D . In [26], these two parameters were determined from the ${}^3\text{H}$ binding energy and the ${}^2a_{nd}$ scattering length. In that paper, a detailed study of 3- and 4-nucleon observables including this 3NF was performed. The role of the 3NF increases with increasing energy, as exemplified in Fig. 5, where the minimum of the differential cross section for nd scattering at 65 MeV is shown. It is clearly visible that the calculation without 3NF badly misses the data. I should stress again that the solid curve including the 3NF is a prediction since all parameters have been fixed before.

In Fig. 6, the tensor analyzing powers T_{20} and T_{22} for elastic pd scattering at 70 MeV are shown [27, 28]. While T_{20} is well described by the NNLO calculation, one observes some visible differences in T_{22} . It is conceivable that this will be cured by the N³LO 3NFs, which are presently worked out. We believe that these corrections to the 3NF are free of LECs, that means even at N³LO one has only two parameters to completely pin down the chiral 3NF. There is also a large amount of pd break-up data, for a detailed comparison between theory and experiment, see [26]. For illustration, in Fig. 7 the break-up cross section in the symmetric space-star configuration as well as the analyzing power are shown, in comparison to the conventional approach based on two high-precision NN potentials and two available phenomenological 3NFs. In [26], we also solved the Yakubowsky equations

Figure 5. Differential cross section for nd scattering at 65 MeV around the minimum at $\theta \simeq 130^\circ$. Solid (dashed) line: NNLO prediction with (without) 3NF. The dot-dashed line gives the prediction based on the CD-Bonn potential without 3NF.

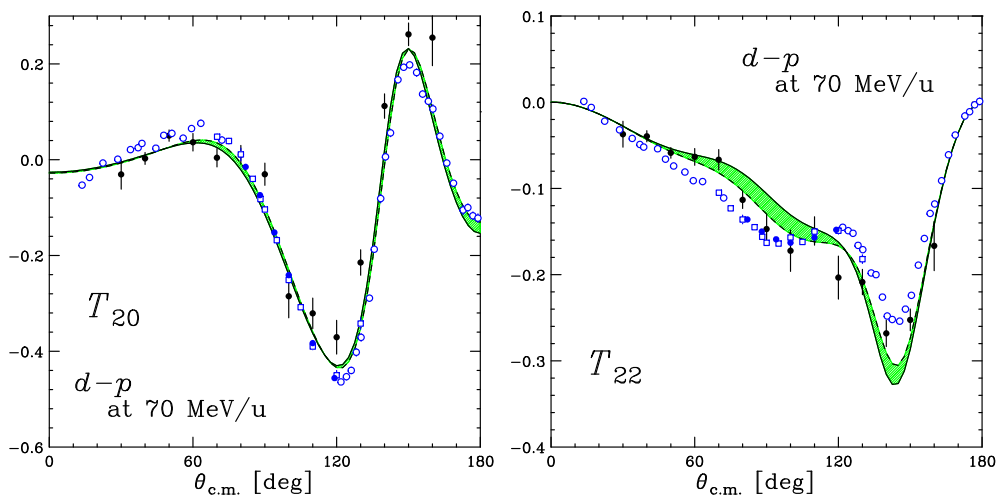
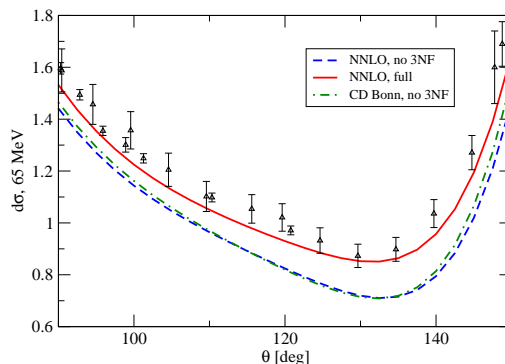


Figure 6. Left: Tensor analyzing powers T_{20} (left) and T_{22} (right) in pd scattering at 70 MeV recently measured at RIKEN [28]. The green band shows the NNLO calculation.

to determine the binding energy (BE) of the α -particle. One finds (all numbers in MeV):

$$\text{NNLO} : \text{BE}(^4\text{He}) = -29.98 \dots - 29.51 , \quad \text{Exp.} : \text{BE}(^4\text{He}) = -29.8 \pm 0.1 , \quad (18)$$

where the experimental value is the “synthetic” binding energy for pure np forces to allow for a direct comparison with the then available chiral EFT forces (for details see [26]). There has also been some more recent work on the isospin dependence of the three-nucleon force and its effect on the binding in the 3-nucleon system [30, 31].

7. RESONANCE SATURATION OF FOUR-NUCLEON COUPLINGS

In the meson sector of CHPT it has been demonstrated that the numerical values of the pertinent NLO LECs L_i can be understood to a high precision by integrating out heavy mesons of all types from the theory [32, 33]. This was coined resonance saturation. For the dimension two and some dimension three LECs of the pion-nucleon sector, these ideas were extended in [34] and later used in studies of neutral pion electroproduction off protons. It thus appears natural to confront the four-nucleon

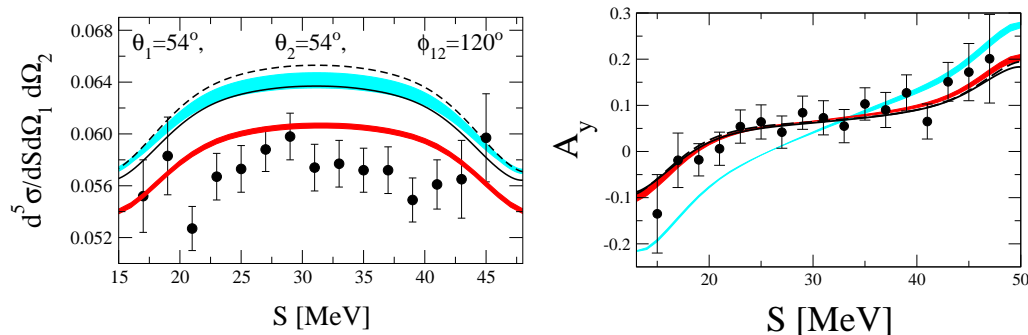


Figure 7. Left: pd breakup cross section data in $[\text{mb MeV}^{-1} \text{sr}^{-2}]$ along the kinematical locus S (in MeV) at 65 MeV. The data are from [29]. NNLO predictions (dark shaded band) and NLO (light shaded band) compared to the conventional NN forces+TM 3NF predictions. The solid (dashed) line refers to the AV18+URBANA IX (CD Bonn+TM') results. Right: Analyzing power.

LECs determined from nuclear EFT with the highly successful phenomenological/meson exchange models of the nuclear force following the lines of Ref. [35] and extending the ideas of resonance saturation to this sector. To be specific, consider some genuine one-boson-exchange (OBE) models. In these models the long range part of the interaction is given by OPE (including a pion-nucleon form factor) whereas shorter distance physics is expressed as a sum over heavier meson-exchange contributions:

$$V_{\text{NN}} = V_{\pi} + \sum_{M=\sigma,\rho,\dots} V_M . \quad (19)$$

Here some mesons can be linked to real resonances (like e.g. the ρ -meson) or are parameterizations of certain physical effects, e.g. the light scalar-isoscalar σ -meson is needed to supply the intermediate range attraction (but it is *not* a resonance). The corresponding meson-nucleon vertices are given in terms of one (or two) coupling constant(s) and corresponding form factor(s), characterized by some cut-off scale. These form factors are needed to regularize the potential at small distances (large momenta) but they should not be given a physical interpretation. As depicted in Fig.7 (left panel) for nucleon momentum transfer below the masses of the exchanged mesons, one can interpret such exchange diagrams as a sum of local operators with increasing number of derivatives (momentum insertions). This is explained in detail in Ref. [35]. In that work the short-range part of different phenomenological potential models was power expanded and the resulting contact operators were compared with the ones in the EFT approach. The latter have to be corrected by adding the corresponding power expanded TPE contributions, which are not present in most phenomenological models. It was then demonstrated explicitly that the values of the LECs C_i determined from various phenomenological OBE models are close to the values found in EFT at NLO and NNLO, see Fig. 7. This was repeated in [17] utilizing spectral function regularization with a similar outcome - the LECs appearing in the chiral EFT fits can be well represented by heavy meson exchanges.

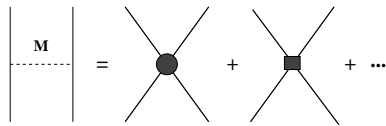
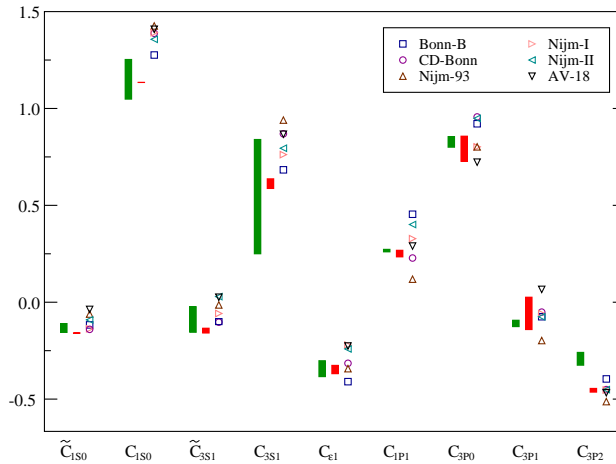


Figure 8: Top: Heavy meson exchange represented as a sum of local interactions with increasing number of derivatives. Right: Comparison of the NLO (green bands) and NNLO (red bands) LECs with values obtained from accurate potentials [35].



8. QUARK MASS DEPENDENCE OF THE NUCLEAR FORCES

Because of the smallness of the up and down quark masses, one does not expect significant changes in systems of pions or pions and one nucleon when the quark masses are set to zero (with the exception of well understood chiral singularities like e.g. in the pion radius or the nucleon polarizabilities). The situation is more complicated for systems of two (or more) nucleons, as first discussed in EFT in [36]. Here, I report on similar work [37] that is mostly concerned with the properties of the deuteron and the S-wave scattering lengths as a function of the quark (pion) mass. These questions are not only of academic interest, but also of practical use for interpolating results from lattice gauge theory. E.g. the S-wave scattering lengths have been calculated on the lattice using the quenched approximation [38]. Another interesting application is related to imposing bounds on the time-dependence of some fundamental coupling constants from the NN sector, as discussed in [39]. To address this issue, at NLO the following contributions have to be accounted for (in addition to the LO OPE and contact terms without derivatives): i) contact terms with two derivatives or one M_π^2 -insertion, ii) renormalization of the OPE, iii) renormalization of the contact terms, and iv) two-pion exchange (TPE). This induces *explicit* and *implicit* quark mass dependences. In the first category are the pion propagator that becomes Coulomb-like in the chiral limit or the M_π^2 corrections to the leading contact terms. These are parameterized by the LECs $\bar{D}_{S,T}$ at NLO. These LECs can at present only be estimated using dimensional analysis and resonance saturation [35]. The implicit pion mass dependence enters at NLO through the pion-nucleon coupling constant (note that the quark mass dependence of the nucleon mass only enters at NNLO) expressed through the pion mass dependence of g_A/F_π in terms of the quantity

$$\Delta = \left(\frac{g_A^2}{16\pi^2 F_\pi^2} - \frac{4}{g_A} \bar{d}_{16} + \frac{1}{16\pi^2 F_\pi^2} \bar{l}_4 \right) (M_\pi^2 - \tilde{M}_\pi^2) - \frac{g_A^2 \tilde{M}_\pi^2}{4\pi^2 F_\pi^2} \ln \frac{\tilde{M}_\pi}{M_\pi}. \quad (20)$$

Here \bar{l}_4 , \bar{d}_{18} and \bar{d}_{16} are LECs related to pion and pion-nucleon interactions, and the value of the pion mass is denoted by \tilde{M}_π in order to distinguish it from the physical one denoted by M_π . In particular, \bar{d}_{16} has been determined in various fits to describe $\pi N \rightarrow \pi\pi N$ data, see [40]. The deuteron BE as a function of the pion mass is shown in Fig.9, we find

that the deuteron is stronger bound in the chiral limit (CL) than in the real world,

$$B_D^{\text{CL}} = 9.6 \pm 1.9 \begin{matrix} +1.8 \\ -1.0 \end{matrix} \text{ MeV} , \quad (21)$$

where the the first indicated error refers to the uncertainty in the value of \bar{D}_{3S_1} and \bar{d}_{16} being set to its average value while the second indicated error shows the additional uncertainty due to the uncertainty in the determination of \bar{d}_{16} . We find no other bound

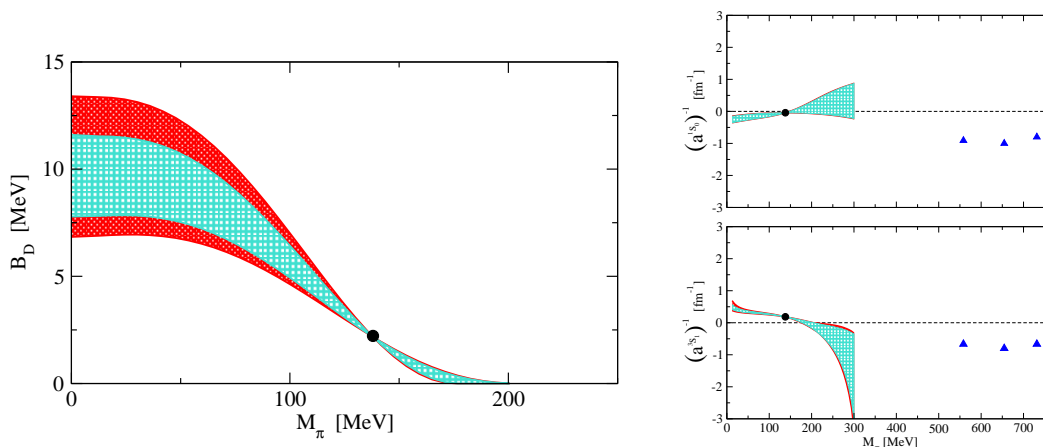


Figure 9. Left panel: Deuteron BE versus the pion mass. The shaded areas show allowed values. The light shaded band corresponds to our main result with the uncertainty due to the unknown LECs $\bar{D}_{S,T}$. The dark shaded band gives the additional uncertainty due to the uncertainty of \bar{d}_{16} . The heavy dot shows the BE for the physical case $\tilde{M}_\pi = M_\pi$. Right panel: The inverse S-wave scattering lengths as functions of \tilde{M}_π . The shaded areas represent the allowed values according to our analysis. The heavy dots corresponds to the values in the real world. The triangles refer to lattice QCD results from [38].

states, although the higher $S = 1$ partial waves rise linear with momentum due to the Coulomb-like pion propagator. Last but not least, we found smaller (in magnitude) and more natural values for the two S-wave scattering lengths in the chiral limit,

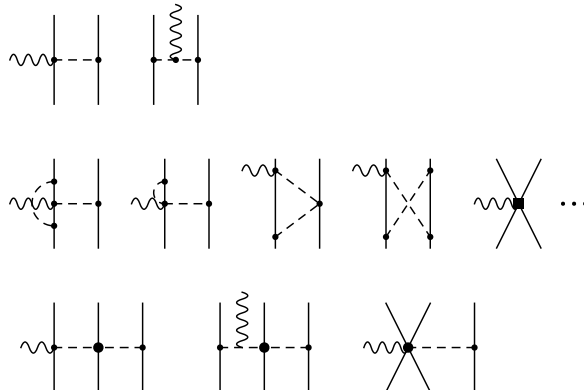
$$a_{\text{CL}}(^1S_0) = -4.1 \pm 1.6 \begin{matrix} +0.0 \\ -0.4 \end{matrix} \text{ fm} , \quad \text{and} \quad a_{\text{CL}}(^3S_1) = 1.5 \pm 0.4 \begin{matrix} +0.2 \\ -0.3 \end{matrix} \text{ fm} . \quad (22)$$

As stressed in [37], one needs lattice data for pion masses below 300 MeV to perform a stable interpolation to the physical value of M_π , cf the right panel in Fig. 9. We conclude that nuclear physics in the chiral limit is much more natural than in the real world. Another interesting application of the quark mass of the nuclear forces is the recently conjectured infrared renormalization group limit cycle in the three-nucleon system [41].

9. BRIEF SUMMARY AND OUTLOOK

From the previous sections it should have become obvious that few-nucleon systems can be studied in chiral effective field theory in a systematic and model-independent way. The

Figure 10: $2N$ and $3N$ currents. First row: Leading pion exchange graphs. Second row: Corrections of various ranges. Third row: $3N$ currents. Solid, dashed, and wiggly lines represent nucleons, pions and photons, in order. Only some representative diagrams are depicted.



two-nucleon system has been analyzed at $N^3\text{LO}$ and accurate results for the deuteron and scattering observables have been obtained. Furthermore, $3N$, $4N$ and even $6N$ systems [42] have been studied at $N^2\text{LO}$. For the first time, the chiral three-nucleon force has been consistently included and the results to this order look very promising. Many other applications have also been performed (some times using the so-called hybrid approach which utilizes the kernel from EFT and wave functions from semi-phenomenological potentials). I mention just a few here: pion-deuteron scattering [43], neutral pion photo- and electroproduction on the deuteron [44][45], Compton scattering off deuterium [46], nuclear parity violation [47] or solar fusion and the *hep* process [48]. Other interesting developments are related to the lattice, just to name a few examples of recent work: nuclear lattice simulations [49], the two-nucleon potential in partially quenched lattice QCD [50] or the discussion of the size of the lattice required to simulate the two-nucleon system [51].

From my point of view, the following problems should be worked out next:

- To study few-nucleon physics at $N^3\text{LO}$, we have to work out the 3NF and 4NF at this order. It is gratifying to notice that no new six-nucleon contact interactions appear at this order and thus one has large predictive power. Furthermore, the 4NF first appears at this order and is parameter-free. It is expected that this force will be much smaller than the 3NF . Still, it will be interesting to obtain the quantitative size of this force.
- Similarly, the currents corresponding to electroweak probes have to be constructed to the same order. The strength of the chiral EFT approach is the consistency with the forces and the automatic incorporation of gauge symmetry. Lots of work on this problem has already been done by the Korean group [52] (see also [53, 54]). However, most of these results need to be rederived using the method of unitary transformation to make them consistent with the forces. Some pertinent diagrams are shown in Fig. 10. Furthermore, three-nucleon currents have never been considered.

The methods described here pave the way to a precision nuclear physics consistent with the symmetries of QCD and thus offer a sound theoretical foundation for this decade old problem.

ACKNOWLEDGMENTS

It is a pleasure to thank my collaborators on these topics, and particularly Evgeny Epelbaum, Walter Glöckle, Hiroyuki Kamada, Andreas Nogga and Henryk Witala. I am grateful to Evgeny Epelbaum for a careful reading of this manuscript. I also would like to thank the organizers, in particular Björn Jonson, for the invitation and the excellent organization.

REFERENCES

1. M. Taketani, S. Nakamura, and M. Sasaki, *Progr. Theoret. Phys. (Kyoto)* **6** (1951) 581.
2. see http://www.phy.anl.gov/theory/ria/av18_il2_exp.gif.
3. J. Carlson and R. Schiavilla, *Rev. Mod. Phys.* **70** (1998) 743.
4. S. Weinberg, *Phys. Lett. B* **251** (1990) 288; *Nucl. Phys. B* **363** (1991) 3.
5. S. R. Beane, P. F. Bedaque, W. C. Haxton, D. R. Phillips and M. J. Savage, in *Shifman, M. (ed.): *At the frontier of particle physics, vol. 1* (World Scientific, Singapore, 2001) [arXiv:nucl-th/0008064].
6. P. F. Bedaque and U. van Kolck, *Ann. Rev. Nucl. Part. Sci.* **52** (2002) 339 [arXiv:nucl-th/0203055].
7. H. Leutwyler, *Annals Phys.* **235** (1994) 165 [arXiv:hep-ph/9311274].
8. S. Weinberg, in *Lecture Notes in Physics*, Vol. 452 (Springer Verlag, Heidelberg 1995) [arXiv:hep-ph/9412326].
9. V. Bernard, N. Kaiser and U.-G. Meißner, *Int. J. Mod. Phys. E* **4** (1995) 193 [arXiv:hep-ph/9501384].
10. C. Hanhart, U. van Kolck and G. A. Miller, *Phys. Rev. Lett.* **85** (2000) 2905 [arXiv:nucl-th/0004033].
11. U. van Kolck, *Phys. Rev. C* **49** (1994) 2932.
12. V. Bernard, N. Kaiser and U.-G. Meißner, *Nucl. Phys. A* **615** (1997) 483 [arXiv:hep-ph/9611253].
13. N. Fettes, U.-G. Meißner and S. Steininger, *Nucl. Phys. A* **640** (1998) 199 [arXiv:hep-ph/9803266].
14. P. Büttiker and U.-G. Meißner, *Nucl. Phys. A* **668** (2000) 97 [arXiv:hep-ph/9908247].
15. M.C.M. Rentmeester, R.G.E. Timmermans, J.J. de Swart, *Phys. Rev. C* **67** (2003) 044001 [arXiv:nucl-th/0302080].
16. N. Kaiser, R. Brockmann and W. Weise, *Nucl. Phys. A* **625** (1997) 758 [arXiv:nucl-th/9706045].
17. E. Epelbaum, W. Glöckle and U.-G. Meißner, *Eur. Phys. J. A* **19** (2004) 125 [arXiv:nucl-th/0304037]; *Eur. Phys. J. A* **19** (2004) 401 [arXiv:nucl-th/0308010].
18. N. Kaiser, *Phys. Rev. C* **61** (2000) 014003 [arXiv:nucl-th/9910044]; *Phys. Rev. C* **62** (2000) 024001 [arXiv:nucl-th/9912054]; *Phys. Rev. C* **63** (2001) 044010 [arXiv:nucl-th/0101052]; *Phys. Rev. C* **64** (2001) 057001 [arXiv:nucl-th/0107064].
19. M. Chemtob, J. W. Durso and D. O. Riska, *Nucl. Phys. B* **38** (1972) 141.
20. E. Epelbaum, W. Glöckle and U.-G. Meißner, arXiv:nucl-th/0405048, to be published in *Nucl. Phys. A*.
21. N. Fettes and U.-G. Meißner, *Nucl. Phys. A* **693** (2001) 693 [arXiv:hep-ph/0101030].

22. V. G. J. Stoks, R. A. M. Kompl, M. C. M. Rentmeester and J. J. de Swart, Phys. Rev. C **48** (1993) 792.
23. SAID on-line program, R.A. Arndt et al., <http://gwdac.phys.gwu.edu>.
24. D.R. Entem and R. Machleidt, Phys. Lett. B **524** (2002) 93 [arXiv:nucl-th/0108057]; Phys. Rev. C **68** (2003) 041001 [arXiv:nucl-th/0304018].
25. J. L. Friar, D. Hüber and U. van Kolck, Phys. Rev. C **59** (1999) 53 [arXiv:nucl-th/9809065].
26. E. Epelbaum, U.-G. Meißner, W. Glöckle and C. Elster, Phys. Rev. C **66** (2002) 064001 [arXiv:nucl-th/0208023].
27. K. Sekiguchi *et al.*, Phys. Rev. C **70** (2004) 014001 [arXiv:nucl-ex/0404026].
28. K. Sekiguchi, *private communication*, and to be published.
29. J. Zejma *et al.*, Phys. Rev. C **55** (1997) 42.
30. E. Epelbaum, U.-G. Meißner and J. E. Palomar, arXiv:nucl-th/0407037.
31. J. L. Friar, G. L. Payne and U. van Kolck, arXiv:nucl-th/0408033.
32. G. Ecker, J. Gasser, A. Pich and E. de Rafael, Nucl. Phys. B **321** (1989) 311; G. Ecker, J. Gasser, H. Leutwyler, A. Pich and E. de Rafael, Phys. Lett. B **223** (1989) 425.
33. J. F. Donoghue, C. Ramirez and G. Valencia, Phys. Rev. D **39** (1989) 1947.
34. V. Bernard, N. Kaiser and U.-G. Meißner, Nucl. Phys. A **615** (1997) 483 [arXiv:hep-ph/9611253].
35. E. Epelbaum, U.-G. Meißner, W. Glöckle and C. Elster, Phys. Rev. C **65** (2002) 044001 [arXiv:nucl-th/0106007].
36. S.R. Beane, P. F. Bedaque, M. J. Savage and U. van Kolck, Nucl. Phys. A **700** (2002) 377 [arXiv:nucl-th/0104030].
37. E. Epelbaum, Ulf-G. Meißner, and W. Glöckle, Nucl. Phys. A **714** (2003) 535 [arXiv:nucl-th/0207089]; nucl-th/0208040
38. M. Fukugita, Y. Kuramashi, M. Okawa, H. Mino and A. Ukawa, Phys. Rev. D **52** (1995) 3003 [arXiv:hep-lat/9501024].
39. S. R. Beane and M. J. Savage, Nucl. Phys. A **713**, 148 (2003) [arXiv:hep-ph/0206113].
40. N. Fettes, V. Bernard, and Ulf-G. Meißner, Nucl. Phys. A **699**, 269 (2000); N. Fettes, doctoral thesis, published in *Berichte des Forschungszentrum Jülich*, **3814**, (2000).
41. E. Braaten and H. W. Hammer, Phys. Rev. Lett. **91** (2003) 102002 [arXiv:nucl-th/0303038].
42. A. Nogga *et al.*, Nucl. Phys. A **737** (2004) 236.
43. S. R. Beane, V. Bernard, E. Epelbaum, U.-G. Meißner and D. R. Phillips, Nucl. Phys. A **720** (2003) 399 [arXiv:hep-ph/0206219].
44. S. R. Beane, V. Bernard, T. S. H. Lee, U.-G. Meißner and U. van Kolck, Nucl. Phys. A **618** (1997) 381 [arXiv:hep-ph/9702226].
45. H. Krebs, V. Bernard and U.-G. Meißner, Nucl. Phys. A **713** (2003) 405 [arXiv:nucl-th/0207072]; arXiv:nucl-th/0405006, accepted for publication in *Eur. Phys. J. A*.
46. R. P. Hildebrandt, H. W. Griesshammer, T. R. Hemmert and B. Pasquini, Eur. Phys. J. A **20** (2004) 293 [arXiv:nucl-th/0307070]; R. P. Hildebrandt, H. W. Griesshammer and T. R. Hemmert, Eur. Phys. J. A **20** (2004) 329 [arXiv:nucl-th/0308054]; S. R. Beane, M. Malheiro, J. A. McGovern, D. R. Phillips and U. van Kolck, arXiv:nucl-th/0403088.

47. S. L. Zhu, C. M. Maekawa, B. R. Holstein, M. J. Ramsey-Musolf and U. van Kolck, arXiv:nucl-th/0407087.
48. T. S. Park *et al.*, Phys. Rev. C **67** (2003) 055206 [arXiv:nucl-th/0208055].
49. D. Lee, B. Borasoy and T. Schäfer, Phys. Rev. C **70** (2004) 014007 [arXiv:nucl-th/0402072].
50. S. R. Beane and M. J. Savage, Phys. Lett. B **535** (2002) 177 [arXiv:hep-lat/0202013].
51. S. R. Beane, P. F. Bedaque, A. Parreno and M. J. Savage, Phys. Lett. B **585** (2004) 106 [arXiv:hep-lat/0312004].
52. T. S. Park, D. P. Min and M. Rho, Phys. Rept. **233** (1993) 341 [arXiv:hep-ph/9301295]; Nucl. Phys. A **596** (1996) 515 [arXiv:nucl-th/9505017].
53. M. Walzl and U.-G. Meißner, Phys. Lett. B **513** (2001) 37 [arXiv:nucl-th/0103020].
54. D. R. Phillips, Phys. Lett. B **567** (2003) 12 [arXiv:nucl-th/0304046].